communications earth & environment

Article

A Nature Portfolio journal

https://doi.org/10.1038/s43247-026-03834-z

Flash droughts amplify maize yield losses through intensified atmospheric aridity

Check for updates

Cancan Qiao [1], Shuo Wang [1,2] ✉, Peng Zhu [3], Jason A. Otkin [4], Zong-Liang Yang [5] & Amir AghaKouchak [6,7,8]

Rapidly intensifying flash droughts during the growing season pose a critical threat to global food security. However, how their impacts on crop yields differ from traditional slow-onset droughts and the underlying mechanisms remain inadequately quantified. Here, by integrating long-term yield records, phenological observations, and reanalysis datasets, we show that flash droughts cause widespread maize yield losses across the United States, with a yield sensitivity 27.53% (19.85–36.53%) greater than that of slow-onset droughts. We further demonstrate that this amplified sensitivity is primarily associated with intensified atmospheric aridity during flash droughts, particularly when flash drought development coincides with critical phenological stages. Yet most process-based crop models systematically underestimate this yield sensitivity, likely due to their insufficient representation of rapid soil moisture depletion. Although irrigation can partially mitigate yield losses, it remains unable to fully buffer crops from flash droughts. Our findings underscore the need to improve crop model fidelity and develop targeted strategies for agricultural resilience against flash droughts.

Droughts have become more frequent in recent decades, accompanied by a growing shift toward flash droughts characterized by the rapid onset of soil moisture deficits[1–4]. Flash droughts occur primarily during the growing season[5–7], where their rapid onset impedes early warning and preparedness, resulting in substantial agricultural and economic losses[5,8,9]. For instance, the 2012 flash drought across the central United States (U.S.) affected approximately 80% of U.S. agricultural land[10,11], causing widespread crop failures, particularly for maize and soybean[12], and incurring over $30 billion in agricultural losses[12]. Similarly, the flash drought that struck Russia in 2010 reduced wheat yields by over 70% in the country's wheat-producing oblasts, triggering a sharp decline in global wheat stocks[13]. Furthermore, Russia's ban on agricultural exports, a policy decision linked to this event, increased food prices in Syria, thereby exacerbating the social and economic tensions that led to the outbreak of civil war[14]. Comparable events have recently been documented across diverse regions, such as Australia[15], China[16,17], Africa[18], and southeastern South America[19]. Despite this projected global increase, especially over cropland[4,20], the impacts of flash droughts on food security and the mechanisms underlying their effects remain poorly constrained.

Soil moisture is a primary regulator of plant water availability, exerting direct control over vegetation dynamics and crop productivity[21,22]. During flash droughts, the rapid depletion of soil moisture impairs critical plant physiological functions, including stomatal conductance, photosynthesis, and biomass assimilation[23–25], with prolonged duration further intensifying plant stress[26]. While initially driven by precipitation deficits, flash droughts are exacerbated by elevated evaporative demand and high temperatures[27–29]. Collectively, these compound hydrometeorological anomalies would reduce ecosystem resistance to flash droughts compared to slow-onset events[30]. Despite growing recognition of flash drought ecological risks[30–32], the impacts of flash droughts on crop yields, particularly the differences from slow-onset droughts, remain poorly quantified. This knowledge gap is critical given the high vulnerability of agriculture to climate change and its fundamental role in global food security. Existing studies are often limited to case-specific analyses[13,19] or ecological proxies like Gross Primary Productivity

[1]State Key Laboratory of Climate Resilience for Coastal Cities, Department of Land Surveying and Geospatial Science, The Hong Kong Polytechnic University, Hong Kong SAR, China. [2]Otto Poon Research Institute for Climate-Resilient Infrastructure, Research Institute for Land and Space, The Hong Kong Polytechnic University, Hong Kong SAR, China. [3]Department of Geography, The University of Hong Kong, Hong Kong SAR, China. [4]Cooperative Institute of Meteorological Satellite Studies, Space Science and Engineering Center, University of Wisconsin–Madison, Madison, WI, USA. [5]Department of Geological Sciences, The John A. and Katherine G. Jackson School of Geosciences, University of Texas at Austin, Austin, TX, USA. [6]Department of Civil and Environmental Engineering, University of California, Irvine, CA, USA. [7]Department of Earth System Science, University of California, Irvine, CA, USA. [8]Institute for Water, Environment and Health, United Nations University, Richmond Hill, ON, Canada. ✉e-mail: shuo.s.wang@polyu.edu.hk

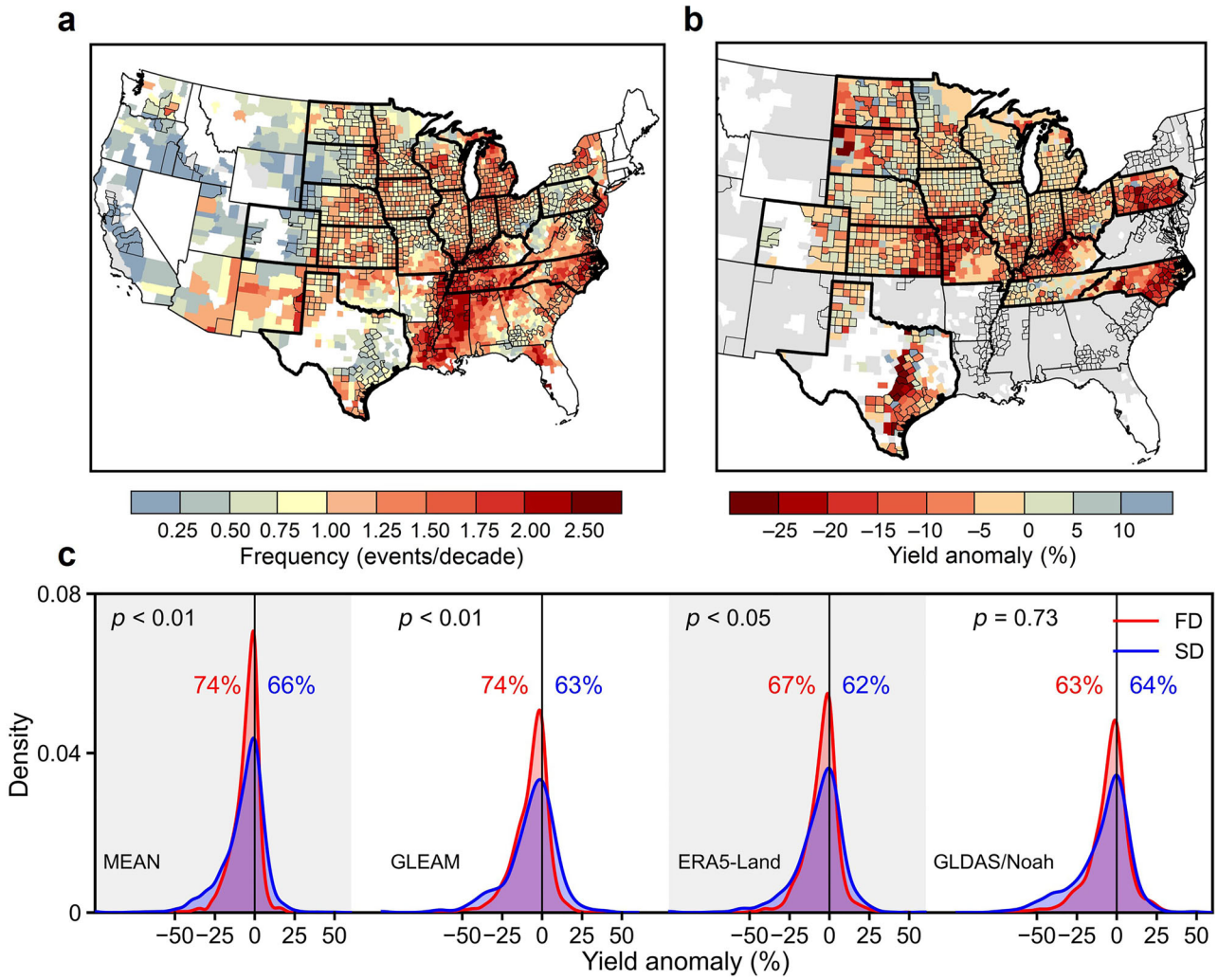

Fig. 1 | Spatial distribution of flash drought frequency and associated maize yield anomalies. a County-level flash drought frequency during the local maize growing season from 1981 to 2023, averaged across the GLEAM, ERA5-Land, and GLDAS/Noah datasets. Bold black outlines indicate the top 18 maize-producing states, while thin black borders delineate the top 50% of maize-producing counties. **b** Spatial distribution of maize yield anomalies (%) during flash drought years, shown as the ensemble mean across datasets. Gray shading represents maize-cultivated counties. **c** Probability density distributions of maize yield anomalies during flash drought (FD) and slow-onset drought (SD) years across the 18 producing states. Vertical lines indicate zero anomaly. The proportion of counties with negative yield anomalies is shown for FD (red) and SD (blue). The significance of their differences was assessed using a one-tailed two-proportion z-test[82]. Exact p values are $p = 1.29 \times 10^{-5}$ for MEAN, $p = 2.13 \times 10^{-8}$ for GLEAM, $p = 0.022$ for ERA5-Land, and $p = 0.73$ for GLDAS/Noah.

(GPP)[24,33], which offer limited insight into actual yield losses. Moreover, as the crop-climate relationships are strongly modulated by growth stage, an assessment across the entire crop life cycle is essential[34,35].

Here, we investigate the impacts of flash and slow-onset droughts on maize yield in the United States, the world's largest maize producer, accounting for over 30% of global production. By integrating long-term (1981–2023) county-level yield records, phenological observations, and multiple soil moisture datasets (GLEAM, ERA5-Land, and GLDAS/Noah), we identify growing-season droughts and classify them as flash or slow-onset events based on their soil moisture depletion rates ("Methods"). Using an explainable machine learning framework, we quantify maize yield sensitivity to each drought type and uncover the mechanisms underlying the amplified losses associated with flash droughts. We further evaluate the performances of ten process-based crop models in reproducing these responses, and we also demonstrate the limited capacity of irrigation to buffer yield losses under flash droughts. Our findings reveal the disproportionate impacts of flash droughts, advance the understanding of drought-related yield risk, and provide a foundation for more resilient agricultural management.

Results

The impact of flash droughts on maize yield

We identified flash and slow-onset droughts during the maize growing season from 1981 to 2023 using county-specific phenological calendars (see Methods and Supplementary Fig. 1). Flash droughts were widespread across nearly all maize-growing counties, with the highest frequency in the humid central U.S. (Fig. 1a). Our analysis focused on 18 states in this core region, which accounted for over 90% of national maize production in 2023 (Supplementary Fig. 2) and provided the most comprehensive phenological records (Supplementary Fig. 3). We assessed average yield anomalies during drought years using county-level yield statistics from the USDA National Agricultural Statistics Service (see "Methods").

Flash droughts were associated with widespread yield losses (Fig. 1b). Negative yield anomalies occurred in 74% of counties, a significantly greater proportion than the 66% observed during slow-onset droughts based on a

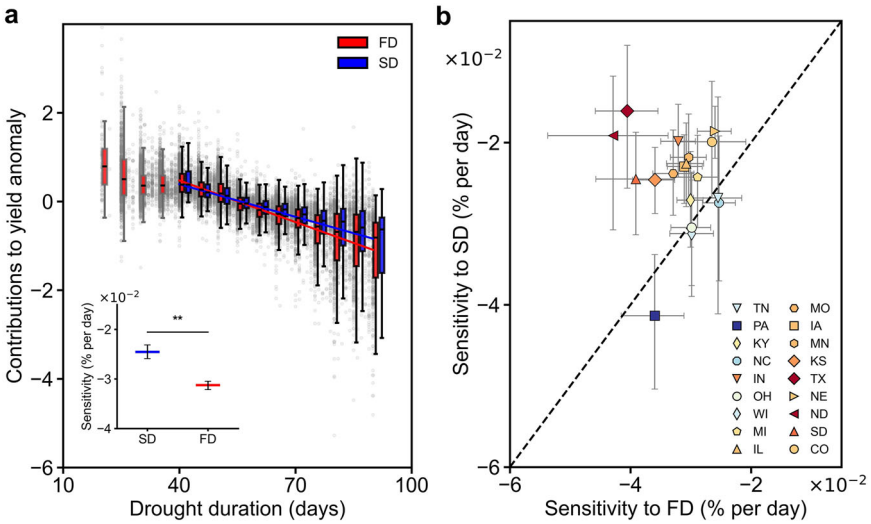

Fig. 2 | Sensitivity of maize yield to flash and slow-onset drought durations. a Partial dependence of yield anomalies on drought duration, estimated using the XGBoost machine learning model integrated with the SHAP framework. Solid red and blue lines indicate the best linear fits for flash (FD) and slow-onset drought (SD) events, respectively. The inset panel displays the corresponding yield sensitivities (% per day), where centre values denote the median regression slopes estimated from 1000 bootstrap samples, and error bars represent the bootstrap-derived 95% confidence intervals. Double asterisks (**) denote statistically significant differences ($p < 0.01$) based on a two-sided Mann–Whitney U test. **b** Comparison of state-level yield sensitivity to flash and slow-onset droughts. Points denote the median regression slopes, and error bars represent the 95% confidence intervals from 1000 bootstrap samples. To enhance clarity and interpretability, sensitivity values are reported as % per 10 days in the main text.

one-tailed two-proportion z-test (Fig. 1c). This indicates that flash droughts impose stronger constraints on crop productivity. A striking example is the 2012 flash drought, which caused severe maize yield reductions in the central U.S. (Supplementary Fig. 4) and triggered exceptionally high crop insurance payouts[36]. Significant yield reductions were also evident across the eastern U.S., a region prone to flash droughts. We conducted separate analyses for each soil moisture dataset and observed broadly consistent results: flash droughts were more likely to cause yield loss than slow-onset droughts. This difference was significant at the 95% confidence level for GLEAM and ERA5-Land (Fig. 1c). While GLDAS/Noah also showed elevated yield loss probabilities for both drought types, the difference was not significant, potentially due to its coarser spatial resolution limiting its detection of rapid soil moisture depletion.

Amplified yield sensitivity to flash droughts

To isolate the impacts of flash and slow-onset droughts on maize yield, we developed an explainable machine learning model using Extreme Gradient Boosting (XGBoost) integrated with Shapley Additive Explanations (SHAP). The model incorporated 22 predictors characterizing yield anomalies during drought years, including drought characteristics, hydrometeorological indicators, agricultural management factors, and fixed effects (Supplementary Fig. 5). Results from fivefold cross-validation across three soil moisture datasets demonstrated the model's efficacy in explaining yield variability ($R^2 = 0.55$–0.66, Supplementary Fig. 6). Here, drought duration was adopted as the primary drought metric because of its intuitive physical representation and its widespread recognition as a preferred IPCC indicator[37]. SHAP values further quantified the marginal contribution of drought duration to yield anomalies. As shown in Fig. 2a, short-duration droughts had negligible or even slightly positive effects on maize yield, whereas longer droughts led to progressively greater yield reductions. These patterns are consistent with previous studies[26,38]. More importantly, at comparable durations, flash droughts generally exhibited stronger yield suppression than slow-onset droughts, as indicated by lower SHAP values. The difference in impact between the two drought types increased with duration.

We further quantified the sensitivity of maize yield to flash and slow-onset drought durations (see Methods). To ensure comparability, only drought events with overlapping duration distributions were included. Across the 18 states, yield sensitivity was −0.312% per 10 days (95% CI: −0.322 to −0.305) for flash droughts ($p < 0.01$) and −0.245% per 10 days (95% CI: −0.259 to −0.231) for slow-onset droughts ($p < 0.01$). The sensitivity to flash droughts exceeded that under slow-onset droughts by 27.53% (95% CI: 19.85 to 36.53%; Fig. 2a). While cross-dataset variations introduced uncertainty in the absolute magnitude of flash drought sensitivity (−0.18% to −0.54% per 10 days), independent analyses with GLEAM, ERA5-Land, and GLDAS/Noah all confirmed its amplification relative to slow-onset droughts (9.8–66.3%, Supplementary Figs. 7–9), reinforcing the robustness of our findings. State-level analyses further indicated consistent patterns in 72.2% of the 18 states (Fig. 2b). The greater difference between yield sensitivity to flash and slow-onset droughts in semi-arid states like North Dakota (ND) and Texas (TX) may be linked to the higher vegetation sensitivity to flash droughts previously observed in drylands[30]. Notably, these states have also experienced substantial maize area expansion over the past four decades, further heightening their vulnerability to flash drought risk.

To test the robustness of our results, we repeated the analyses using alternative flash drought definitions and drought metrics (see "Methods"). Amplified yield sensitivity to flash droughts was consistently observed across various flash drought definitions, with sensitivity to flash droughts exceeding that to slow-onset droughts by 24.23% using the Soil Water Deficit Index (SWDI) definition (Supplementary Fig. 10) and by 21.39–24.24% across different soil moisture percentile-based thresholds (Supplementary Fig. 11). Additionally, the amplified yield sensitivity to flash droughts persisted when drought intensity and drought severity were used as alternative drought metrics in place of drought duration (Supplementary Figs. 12–13).

Mechanisms underlying amplified yield sensitivity to flash droughts

To uncover the mechanisms underlying the amplified sensitivity of maize yield to flash droughts, we first compared key hydrometeorological conditions during flash and slow-onset droughts (Fig. 3). Although both drought types involved comparable soil moisture and precipitation deficits (Fig. 3e, f), maize growth experienced substantially greater atmospheric aridity and higher temperatures during flash droughts (Fig. 3c, d). Specifically, flash droughts were characterized by significant increases in vapor pressure deficit (VPD) and temperature, with median standardized anomalies of 0.630 and 0.354, respectively (Fig. 3a). The corresponding anomalies during slow-onset droughts were 0.489 for VPD and 0.295 for temperature (Fig. 3b). We further applied ridge regression analysis to quantify the relative contributions of the hydrometeorological drivers to the amplified maize yield sensitivity at the state level[39]. The results identified intensified atmospheric aridity, particularly during the drought onset stage, as the primary driver of the amplified sensitivity (Supplementary Fig. 14). Specifically, flash droughts exhibited approximately 50% larger VPD anomalies during the drought onset stage than slow-onset droughts (Supplementary Fig. 15).

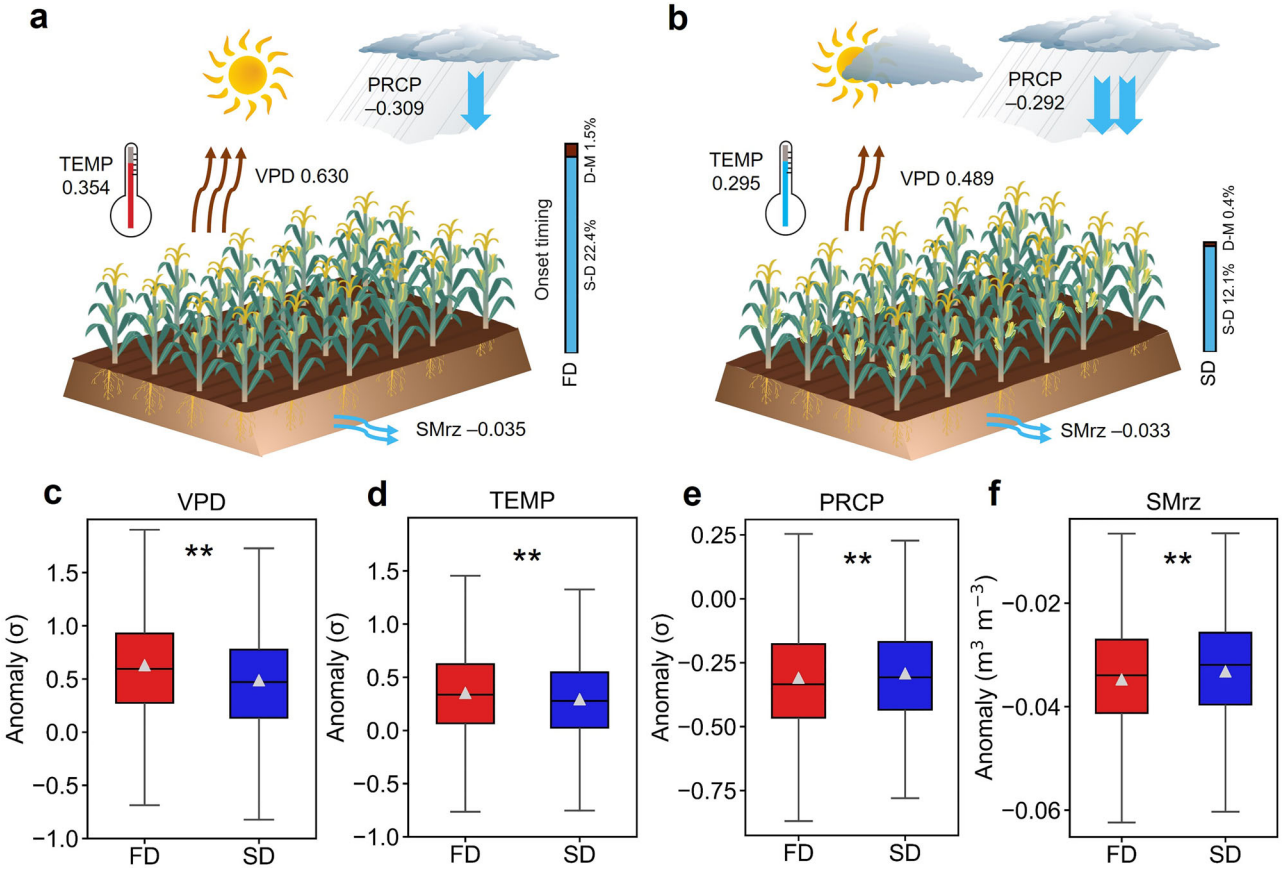

Fig. 3 | Physical mechanisms underlying amplified yield sensitivity to flash droughts. a, b Mean standardized anomalies (σ) of vapor pressure deficit (VPD), temperature (TEMP), precipitation (PRCP), along with mean anomalies of root-zone soil moisture (SMrz, $m^3\ m^{-3}$) during flash drought (FD, $n = 9529$) and slow-onset drought (SD, $n = 3191$) events. Bars within (**a**) and (**b**) show the proportional distribution of drought onset timing across phenological stages for flash and slow-onset droughts, including silk–dough (S–D) and dough–mature (D–M). The plant–silk stage is excluded from the visualization for clarity. **c–f** Comparison of hydrometeorological anomalies during flash and slow-onset droughts. Triangles represent mean values. Double asterisks (**) denote statistically significant differences ($p < 0.01$) based on the two-sided Mann–Whitney U test. Exact p values are $p = 1.16 \times 10^{-40}$ for VPD, $p = 1.60 \times 10^{-11}$ for TEMP, $p = 2.46 \times 10^{-7}$ for PRCP, and $p = 7.03 \times 10^{-13}$ for SMrz. Vector elements used in the figure are adapted from https://ian.umces.edu/media-library/.

Concurrently, elevated temperature anomalies accumulated throughout the entire flash drought period emerged as another important driver by impairing physiological functions and reducing carbon uptake.

We further examined the drought onset phenological timing and stage-specific exposure during the sustained drought condition phase for flash and slow-onset droughts. Compared with slow-onset droughts, flash droughts were more likely to initiate during the early reproductive stages, including the critical silk–dough stage (Fig. 3). Additionally, cross-stage flash droughts exhibited a higher probability of sustained drought exposure during the silk–dough stage than slow–onset droughts (Supplementary Fig. 16). This closer alignment of flash drought development with critical reproductive stages, reflected in both drought onset timing and sustained drought exposure, may collectively amplify maize vulnerability to flash drought stress by reducing the time available for crop adaptation and field responses.

Contrasting effects of flash droughts on maize yield in crop models versus yield statistics

We further examined the sensitivity of maize yield to flash droughts across ten process-based crop models. While all models except LDNDC captured the detrimental effects of droughts, most substantially underestimated yield sensitivity relative to the observational estimates (Fig. 4a). This underestimation was spatially consistent across all states, with inter-model differences generally exceeding inter-state variations (Fig. 4b). These systematic discrepancies suggest potential deficiencies in model structures, particularly in simulating soil water balance and water deficit stress. A review of model documentation indicates that root-zone soil moisture is internally generated by the water-balance modules rather than directly constrained by external observations (Supplementary Table 1). Furthermore, although crop models used a common soil database (HWSD, The Harmonized World Soil Database), their representations of soil layering and soil-water-balance formulations differed substantially[40]. Consequently, the inaccurate simulation of soil moisture dynamics likely contributed to both the underestimated yield sensitivity and the considerable inter-model uncertainty.

Notably, most models similarly underestimated yield sensitivity to both flash and slow-onset droughts, implying that their internal response processes to different drought types were broadly comparable. All crop models consistently reproduced stronger sensitivity under flash droughts than under slow-onset droughts, with EPIC-IIASA and PEPIC showing relatively closer agreement with the observed estimates. However, across most models, the simulated magnitude of this amplified sensitivity was generally weaker than observed. This suggests that the compound stress from rapid soil moisture depletion, intensified atmospheric aridity associated with flash droughts, is only partially represented in the current crop models.

Discussion

Flash droughts have attracted growing scientific and public attention in recent years. While previous studies have primarily examined their hydroclimatic drivers, the agricultural impacts of these events remain

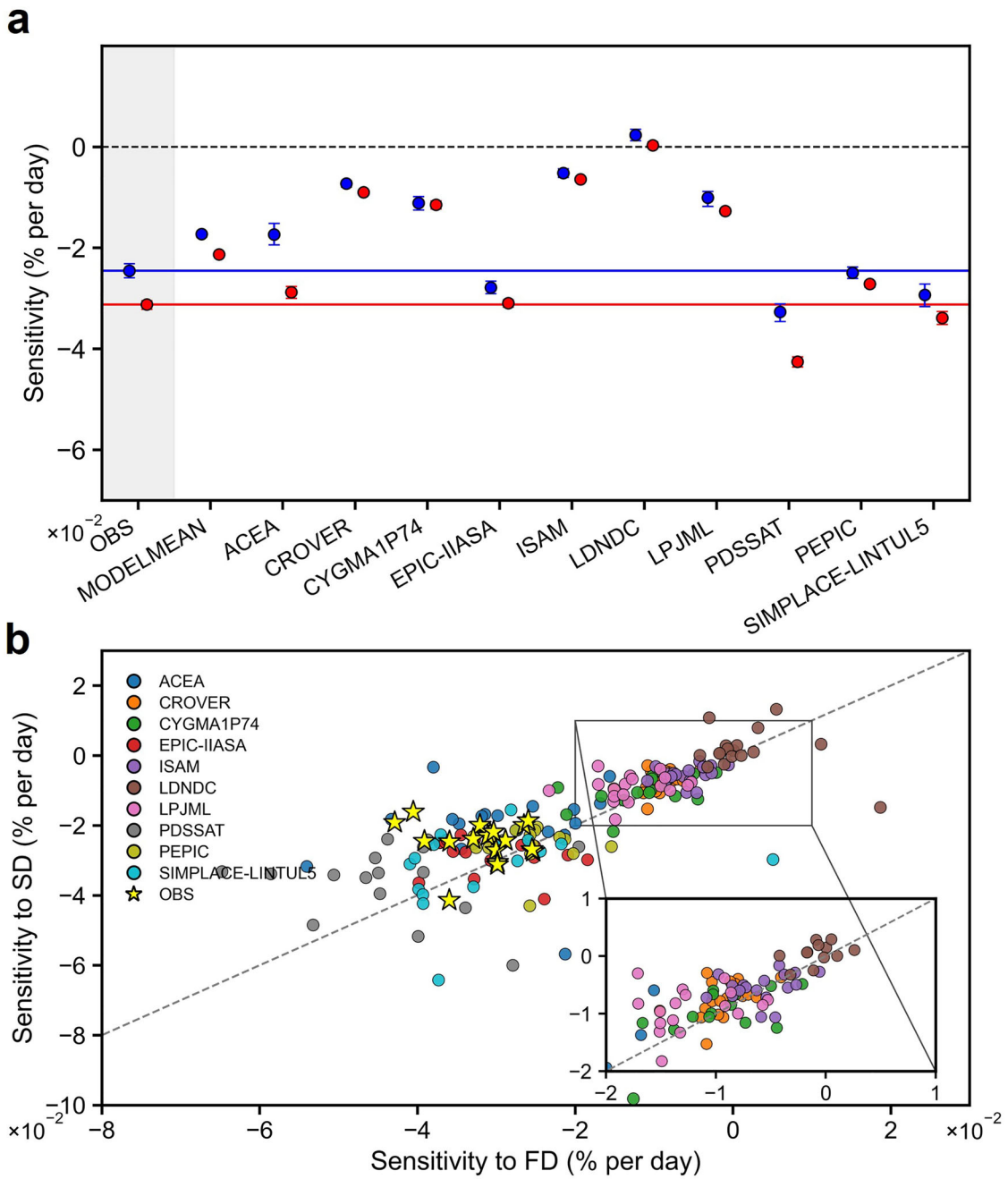

Fig. 4 | Estimates of maize yield sensitivity to flash and slow-onset droughts derived from process-based crop models and yield observations. a Maize yield sensitivity to flash drought (FD; red) and slow-onset drought (SD; blue) estimated from simulations by ten crop models and yield observations (OBS). "MODELMEAN" represents the ensemble mean of multi-crop models. Points denote the median regression slopes estimated from 1000 bootstrap samples, and error bars represent the bootstrap-derived 95% confidence intervals. **b** Comparison of state-level sensitivities to FD and SD between crop models and yield observations across 18 states. Each dot represents one state, and results from the same crop model are shown in the same color. The dashed line indicates the 1:1 reference line.

inadequately quantified, particularly the difference from traditional slow-onset droughts. By integrating agricultural statistics, hydrometeorological data, and an interpretable machine learning model, we demonstrate that U.S. maize yield exhibits an amplified sensitivity to flash droughts compared to slow-onset droughts. We further reveal that the intensified atmospheric aridity associated with flash droughts is the dominant driver of this amplified yield sensitivity, particularly when flash droughts coincide with critical maize growth stages. Recent ecological studies have also highlighted the disproportionate impacts of flash droughts and shown that concurrent atmospheric aridity and extreme heat can further amplify these impacts[30,32,41]. Specifically, intensified atmospheric aridity can trigger stomatal closure, limit photosynthesis, and increase the risk of xylem embolism[30,41], while extreme heat can further impair physiological processes and carbon assimilation[32]. These findings provide an ecological context for our results and support the interpretation that flash droughts amplify yield losses through intensified atmospheric aridity.

Our analysis primarily uses an established indicator for flash droughts based on soil moisture percentile dynamics, defined using a 40–20 threshold. To test the robustness of our findings, we also apply the Soil Water Deficit Index (SWDI), an alternative metric tailored to agriculture[7,42]. Using the SWDI-based metric, we consistently confirm the amplified maize yield sensitivity to flash droughts, with an increase of 24.23% relative to slow-onset droughts (Supplementary Fig. 10), reinforcing the generality of our conclusions. Consistent results are also observed across different soil

moisture percentile thresholds (Supplementary Fig. 11). Specifically, when the percentile thresholds are adjusted from 40–20 to 40–15 and 50–20, the magnitude of amplification decreases slightly from 27.53% to 21.39% and 24.24%, respectively. Although our analysis focuses on U.S. maize due to data availability, field experiments in China have similarly shown that flash droughts can cause greater damage to wheat yields over short periods[43]. Extending such analyses to other crops and regions will require more detailed agricultural data, such as annual crop phenology and irrigation inputs at finer spatiotemporal scales.

Given the critical role of irrigation in mitigating drought impacts[44,45], we examine how flash drought sensitivity varies with irrigation rates across counties in four semi-arid U.S. states (Nebraska, Kansas, Texas, and Colorado) where maize production is heavily irrigated (Supplementary Fig. 17). Our findings confirm that irrigation is an effective on-farm strategy that partially offsets the adverse effects of flash droughts on maize yield (Supplementary Fig. 18a). However, even under high irrigation levels, flash droughts continue to cause stronger yield losses than slow-onset droughts (Supplementary Fig. 18b), a pattern robust across a range of irrigation rate thresholds (≥40% to ≥80%, Supplementary Fig. 19). This limited mitigation potential is likely constrained by irrigation's insufficient relief against the intensified atmospheric aridity and high temperatures of flash droughts (Supplementary Fig. 20). Furthermore, the rapid onset of flash droughts can outpace early warning systems and delay irrigation responses, limiting the protective benefits of even well-equipped systems.

Soil moisture provides a more accurate measure of crop water supply than precipitation[22,46]. However, process-based crop models typically use precipitation as an external input and internally simulate soil moisture using simplified, unconstrained water-balance schemes (Supplementary Table 1). This structural limitation likely causes these models to underestimate maize yield sensitivity to flash droughts, as they fail to capture realistic soil moisture variability[47,48]. Although the ensemble mean of the ten crop models aligns most closely with observed sensitivity, substantial inter-model variability persists, highlighting the need to improve and harmonize crop modeling frameworks[49,50]. Consequently, yield projections from such models should be interpreted with caution, and a balanced integration of process-based and data-driven approaches is essential for robust climate change impact assessments[51].

Different from traditional slow-onset droughts, our study robustly reveals the amplified sensitivity of maize yield to flash droughts using multiple drought metrics and a comprehensive machine learning framework. Yet several caveats warrant consideration. First, while our model accounts for location-fixed effects, it does not explicitly represent specific static factors like fertilizer use, potentially overlooking their influence on drought impacts[25,52]. Second, constrained by data, we used fixed county-level irrigation rates that may not capture temporal variations in infrastructure and management, potentially introducing uncertainty into our estimates of irrigation's mitigating role.

Despite these limitations, our findings provide new evidence that flash droughts induce disproportionately larger agricultural impacts. The amplified sensitivity of flash droughts emphasizes the urgency of improving drought management systems to mitigate crop losses. Effective drought management requires both timely early warning and prospective approaches[53,54]. However, the rapid onset of flash droughts poses a fundamental challenge to current conventional drought management systems[55]. For instance, drought early warning systems (DEWS) widely deployed across much of the United States often struggle to capture flash droughts[56]. In addition, the limited mitigating effect of irrigation under flash droughts suggests that conventional adaptation strategies may be insufficient, highlighting the need for complementary approaches such as the development of drought-resistant crop varieties[57].

Methods

Crop data

The U.S. county-level maize yield and production data from 1981 to 2023 were obtained from the United States Department of Agriculture (USDA) National Agricultural Statistics Service (NASS, https://quickstats.nass.usda.gov/). NASS collects agricultural data through multiple sources, and to ensure consistency, all data used in this study were directly taken from the survey program. NASS also provides the weekly Crop Progress Reports (CPR), which document the cumulative progress of maize phenological stages, namely plant, silk, dough, and mature, expressed as the percentage of planted area reaching each stage at the county or state level[58]. Due to the limited spatial and temporal coverage of county-level reports, we relied on state-level data to derive annual maize phenological dates from 1981 to 2023. For each state, the weekly reported values were interpolated to determine the calendar day on which 50% of the planted area had reached a specific phenological stage, which was then designated as the representative date for that stage[59]. All counties within a given state were assumed to follow the same phenological calendar, and the maize growing season was divided into three key stages: plant to silk (P–S), silk to dough (S–D), and dough to mature (D–M). Finally, maize-specific irrigation rates were obtained from the MIRCA2000 dataset[60] and aggregated to the county level. Based on agricultural census statistics, this dataset provides crop-specific, high-resolution irrigation information and has served as a primary source in recent studies[44,61,62].

Climate data

We used three reanalysis soil moisture datasets to identify flash and slow-onset droughts during the period of 1981–2023, including Global Land Evaporation Amsterdam Model (GLEAM v4.1a, 0.1° resolution)[63], ECMWF Reanalysis (ERA5-Land, 0.1° resolution)[64], and Global Land Data Assimilation System (GLDAS) Noah (0.25° resolution)[65]. For GLEAM and GLDAS/Noah datasets, daily root-zone soil moisture was directly extracted from the variables SMrz and RootMoist_inst, respectively. For ERA5-Land, we aggregated the first three soil moisture layers using weights (0.07, 0.21, and 0.72) to achieve the root-zone averaged soil moisture (1 m depth)[32]. Notably, the root-zone depth of GLEAM comprises three model layers for tall vegetation (0–10, 10–100, and 100–250 cm), two for low vegetation (0–10, 10–100 cm), and one for bare soil (0–10 cm)[66]. In the GLDAS/Noah dataset, root-zone depth for low vegetation is defined as the sum of the top three soil layers (0–100 cm)[67]. For maize, which is represented as low vegetation, the effective root-zone depths in GLEAM and GLDAS/Noah are therefore broadly comparable to the ~1 m soil depth used in ERA5-Land.

Daily temperature and precipitation at 4-km resolution over the same period were obtained from the Parameter-elevation Regressions on Independent Slopes Model (PRISM) to characterize the weather conditions during the maize growing season[68]. The PRISM Group collects meteorological observations from various monitoring networks and has developed an interpolation method that realistically represents climatic patterns across the United States. The PRISM dataset has been extensively validated and is widely used to evaluate climate–crop relationships[34,35,69]. In addition, we calculated daily vapor pressure deficit (VPD) using near-surface temperature and dew point temperature from the PRISM dataset. VPD was defined as the difference between the saturated water vapor pressure, determined by near-surface temperature, and the actual water vapor pressure, derived from dew-point temperature[70].

Flash drought identification

We identified flash and slow-onset droughts at the county scale using a widely adopted indicator based on root-zone soil moisture (SM) percentiles[3,25,28,30,32]. First, daily SM data were aggregated to the pentad scale (5-day intervals) and subsequently converted into percentiles for each calendar pentad from 1981 to 2023. A drought event was defined as beginning when SM percentiles dropped from above the 40th to below the 20th percentile, and ending when values remained above the 20th percentile for two consecutive pentads. Specifically, each drought event was divided into an onset stage (SM decreased from above the 40th to the first occurrence below the 20th percentile) and a drought condition stage (when SM remained below the 20th percentile, see Supplementary Fig. 1). To exclude dry spells with little impacts on crop productivity, SM should remain below

the 20th percentile for at least three pentads[28]. The identified droughts were further classified as flash or slow droughts based on the rate of decline in SM percentiles during the onset stage. For flash droughts, the average declining rate should be at least five percentiles per pentad, whereas slow-onset droughts exhibit a slower rate of decline. To focus on drought events with direct implications for maize growth, we considered only those with both onset and drought condition stages occurring within the growing season.

The key attributes of flash and slow-onset droughts, including duration, intensity, severity, onset timing, and phenological stage-specific exposure, were identified to characterize their distinct features. Drought duration was determined as the total number of days spanning both the onset and drought stages within the growing season[3,30]. Drought intensity was quantified as the mean deviation of SM percentiles below the 40th percentile throughout the drought period[71]. Drought severity was calculated as the cumulative deviation of SM percentiles below the 40th percentile during the drought period, thereby jointly characterizing drought duration and intensity. The onset timing of each drought event was classified according to the phenological stage in which the drought began, providing critical information for early warning and adaptive field management. For drought events spanning multiple phenological stages, we explicitly characterized the phenological stage-specific exposure probability during the sustained drought condition phase. This exposure probability was defined as the proportion of cross-stage events whose sustained drought condition phase overlapped with a specific phenological stage relative to the total number of cross-stage events.

Hydrometeorological indicators

Maize development is influenced by multiple climatic stresses, among which dry stress, heat stress, and heavy rainfall are particularly critical. To isolate the effects of flash droughts, we quantified drought characteristics (duration, intensity, and onset timing) alongside key hydrometeorological indices throughout the growing season. These included extreme degree days (EDD), growing degree days (GDD), maximum 5-day accumulated rainfall (Max5d Rain), total precipitation (PRCP), and vapor pressure deficit (VPD). GDD and EDD were calculated to characterize heat exposure during maize development using the following equations[34]:

$$GDD = \sum_{h=1}^{N} DD_h,\ DD_h = \begin{cases} 0,\ T_h \le T_{base} \\ T_h - T_{base},\ T_{base} < T_h \le T_{opt} \\ T_{opt} - T_{base},\ T_{opt} < T_h \end{cases} \quad (1)$$

$$\mathrm{EDD} = \sum_{h=1}^{N} DD_h,\ DD_h = \begin{cases} 0,\ T_h \le T_{opt} \\ T_h - T_{opt},\ T_{opt} < T_h \end{cases} \quad (2)$$

Here, T_h denotes the hourly surface air temperature, and N is the total number of hours in each maize growing stage (P–S, S–D, and D–M). The temperature thresholds T_{base} and T_{opt} were set at 8 °C and 30 °C, respectively[69]. We also calculated Max5d Rain to represent the contribution of extreme rainfall events. Total PRCP and mean VPD during each growth stage were used to characterize the background hydroclimatic conditions relevant to maize development.

All climate variables were spatially averaged to the county level. To remove long-term trends and emphasize interannual variability, we detrended EDD, GDD, Max5d Rain, PRCP, and VPD using locally weighted scatterplot smoothing (LOESS) with a smoothing span of 0.3. This span was selected to avoid both overfitting short-term fluctuations and excessive smoothing over the relatively long study period (1981–2023)[72]. We additionally tested LOESS spans of 0.2 and 0.4 to support the robustness of the results (Supplementary Figs. 21–22). In contrast, to preserve the full signal of drought events, the original values of drought characteristics, including drought duration, intensity, severity, were retained to better capture their direct impacts on crop productivity.

Sensitivity of maize yield to flash droughts

Before estimating the crop response to flash droughts, we first removed long-term yield trends attributable to technological advances using LOESS[72,73]. We then restricted the yield anomalies and sensitivity assessment to county-year samples that experienced only a single flash or slow-onset drought event during the growing season, enabling a distinct comparison between the two drought types. These samples accounted for over 90% of all drought events (Supplementary Fig. 23), ensuring both the robustness and representativeness of our analysis.

To examine the sensitivity of maize yield to flash and slow-onset droughts, we developed an Extreme Gradient Boosting (XGBoost)[74] model and applied Shapley Additive Explanations (SHAP)[75] for interpretation (Supplementary Fig. 5). As a decision tree-based machine learning approach, the XGBoost model is well-suited for capturing complex relationships while maintaining high predictive performance and interpretability[76]. Specifically, yield anomalies were modeled as the target variable, with predictors including drought characteristics (duration, intensity, and onset timing), hydrometeorological indicators (EDD, GDD, Max5d Rain, PRCP, and VPD), and agricultural management (irrigation rate). To distinguish between drought types, a categorical variable was added to differentiate flash and slow droughts when building models. We split the data into training (80%) and test (20%) subsets. Optimized hyperparameters were selected using the "Optuna" package in Python, and five-fold cross-validation indicated the high efficiency of our XGBoost model with R^2 higher than 0.55.

The XGBoost model outputs were interpreted using the SHAP approach, which combines additive feature attribution with Shapley values derived from cooperative game theory. Larger absolute SHAP values indicate stronger influences on model predictions, with negative and positive values denoting negative and positive contributions, respectively. Importantly, SHAP values quantify the marginal contribution of each predictor to the target variable while accounting for other controlling factors included in the model. In this study, we defined yield sensitivity to flash and slow-onset droughts as the slope of the relationship between a given drought metric and its corresponding SHAP values, with the latter representing the individual contribution of the corresponding drought metric to yield anomalies. Considering that drought duration provides a more intuitive and physically interpretable characterization of drought events, it was adopted as the primary metric in the main analysis. To further assess the robustness of our findings, we additionally evaluated yield sensitivity using drought intensity and drought severity as alternative drought metrics.

Crop model simulation

To evaluate whether crop models can reproduce maize yield responses under flash and slow-onset drought conditions, we compared the yield sensitivities derived from observed maize yields with those derived from historical yield simulation outputs available from the Inter-Sectoral Impact Model Intercomparison Project (ISIMIP). ISIMIP provides standardized simulation protocols and consistent climate forcing inputs[77], thereby facilitating robust inter-model comparison of crop responses to climate variability and extremes[47,78,79]. We evaluated simulated maize yield responses during drought years from ten global gridded crop models (GGCMs), including ACEA, CROVER, CYGMA1p74, EPIC-IIASA, ISAM, LDNDC, LPJmL, pDSSAT, PEPIC, and SIMPLACE-LINTUL5 available within the ISIMIP3a framework. These models simulated historical maize yields (1981–2016) at 0.5° spatial resolution and were driven by the observation-based climate forcing dataset GSWP3-W5E5. Model-specific parameterization, calibration, and validation procedures were conducted by the corresponding modeling groups. More detailed information on model configurations can be found in Supplementary Table 1 and previous studies[62,80].

We quantified simulated maize yield sensitivity to flash and slow-onset droughts using the same XGBoost model combined with the SHAP interpretation framework applied in the observational yield analysis (Supplementary Fig. 5). Specifically, simulated gridded maize yields were first

aggregated to the county level as the weighted sum of rainfed and irrigated yields[79], with weights derived from the corresponding rainfed and irrigated harvested areas from the MIRCA dataset. County-level simulated yield anomalies were then calculated by removing long-term yield trends using the LOESS method, and were used as the target variable in the XGBoost model. Predictor variables included drought characteristics, hydrometeorological indicators, agricultural management factors, and fixed effects. Notably, hydrometeorological indicators were recalculated from the GSWP3-W5E5 climate forcing dataset used to drive the GGCM simulations, thereby maintaining consistency between simulated yields and climate inputs. Separate XGBoost models with SHAP interpretation were constructed for each crop model individually. Simulated yield sensitivity under flash and slow-onset droughts was then quantified based on the relationship between drought duration and the corresponding SHAP values.

Robust checks

To strengthen the robustness of our analysis, we conducted a series of robustness tests. First, we varied the initial threshold for identifying flash droughts by adjusting the SM percentile from the 40th to the 50th percentile. We also tested the effect of modifying the drought termination threshold by lowering the SM percentile from the 20th to the 15th percentile (Supplementary Fig. 11). Beyond percentile-based definitions, we further applied a recently developed method for detecting flash droughts based on the Soil Water Deficit Index (SWDI, Supplementary Fig. 10). SWDI is derived from soil moisture (θ) and key hydraulic properties, specifically the field capacity (θ_{FC}) and the permanent wilting point (θ_{WP}), which were calculated separately for each soil moisture dataset[42,81].

$$SWDI = \left(\frac{\theta - \theta_{FC}}{\theta_{FC} - \theta_{WP}}\right) \times 10 \quad (3)$$

The SWDI equals zero when soil moisture is at the field capacity, and −10 when it reaches the wilting point with no available water for plants. Negative SWDI values indicate soil water deficit. According to this method, flash droughts are identified by a rapid decline in SWDI from above −3 to below −5 within 20 days (or four pentads), with SWDI remaining below −5 for at least three consecutive pentads thereafter[7]. In contrast, droughts with an onset development period exceeding four pentads are classified as slow-onset droughts.

Reporting summary

Further information on research design is available in the Nature Portfolio Reporting Summary linked to this article.

Data availability

All data used in this study are publicly available. US maize yield, production, and Crop Progress Report are obtained from https://quickstats.nass.usda.gov/. The PRISM daily spatial climate dataset is available at https://prism.oregonstate.edu/. The maize irrigated and rainfed area data are available at https://www.uni-frankfurt.de/45218031/data_download. The GLEAM soil moisture dataset is available at https://www.gleam.eu/. The ERA5-Land soil moisture dataset is available at https://cds.climate.copernicus.eu/datasets/reanalysis-era5-land?tab=download. The GLDAS/Noah soil moisture dataset is available at https://disc.sci.gsfc.nasa.gov/datasets?keywords=GLDAS. The ISIMIP crop model yield simulations and the GSWP3-W5E5 climate forcing data are available through the ISIMIP data portal at https://data.isimip.org/search/tree/ISIMIP3a/. The source data used to reproduce the findings of this study are available at https://doi.org/10.5281/zenodo.21219421.

Code availability

The code used for this study is available at https://doi.org/10.5281/zenodo.21219421.

Received: 8 January 2026; Accepted: 12 July 2026;
Published online: 29 July 2026

References

1. Dai, A. Increasing drought under global warming in observations and models. *Nat. Clim. Change* **3**, 52–58 (2013).
2. Christian, J. I. et al. Global distribution, trends, and drivers of flash drought occurrence. *Nat. Commun.* **12**, 6330 (2021).
3. Yuan, X. et al. A global transition to flash droughts under climate change. *Science* **380**, 187–191 (2023).
4. Christian, J. I. et al. Global projections of flash drought show increased risk in a warming climate. *Commun. Earth Environ.* **4**, 1–10 (2023).
5. Otkin, J. A. et al. Flash Droughts: A review and assessment of the challenges imposed by rapid-onset droughts in the United States. *Bull. Am. Meteorol. Soc.* **99**, 911–919 (2018).
6. Ford, T. W. et al. Flash drought indicator intercomparison in the United States. *J. Appl. Meteor. Climatol.* **62**, 1713–1730 (2023).
7. Lovino, M. A., Pierrestegui, M. J., Müller, O. V., Müller, G. V. & Berbery, E. H. The prevalent life cycle of agricultural flash droughts. *NPJ Clim. Atmos. Sci.* **7**, 1–11 (2024).
8. Pendergrass, A. G. et al. Flash droughts present a new challenge for subseasonal-to-seasonal prediction. *Nat. Clim. Change* **10**, 191–199 (2020).
9. Mohammadi, K., Jiang, Y. & Wang, G. Flash drought early warning based on the trajectory of solar-induced chlorophyll fluorescence. *Proc. Natl. Acad. Sci. USA* **119**, e2202767119 (2022).
10. Otkin, J. A. et al. Assessing the evolution of soil moisture and vegetation conditions during the 2012 United States flash drought. *Agr. For. Meteorol*. **218–219**, 230–242 (2016).
11. Woloszyn, M. et al. *Flash Drought: Current Understanding and Future Priorities; Report of the 2020 NIDIS Flash Drought Virtual Workshop*. (NOAA National Integrated Drought Information System, 2021).
12. Smith, A. B. U.S. *Billion-dollar Weather and Climate Disasters, 1980–present (NCEI Accession 0209268)*. https://doi.org/10.25921/STKW-7W73 (NOAA National Centers for Environmental Information, 2020).
13. Hunt, E. et al. Agricultural and food security impacts from the 2010 Russia flash drought. *Weather Clim. Extrem.* **34**, 100383 (2021).
14. Gleick, P. H. Water, drought, climate change, and conflict in Syria. **6**, 331–340 (2014).
15. Nguyen, H. et al. Using the evaporative stress index to monitor flash drought in Australia. *Environ. Res. Lett.* **14**, 064016 (2019).
16. Fu, K. & Wang, K. Quantifying flash droughts over China from 1980 to 2017. *J. Geophys. Res. Atmosph.* **127**, e2022JD037152 (2022).
17. Wang, Y. & Yuan, X. Anthropogenic speeding up of south China flash droughts as exemplified by the 2019 Summer-Autumn transition season. *Geophys. Res. Lett.* **48**, e2020GL091901 (2021).
18. Yuan, X., Wang, L. & Wood, E. F. Anthropogenic intensification of Southern African flash droughts as exemplified by the 2015/16 season. *Bull. Am. Meteorol. Soc.* **99**, S86–S90 (2018).
19. Lovino, M. A. et al. Agricultural flash droughts and their impact on crop yields in southeastern South America. *Environ. Res. Lett.* **20**, 054058 (2025).
20. Mahto, S. S. & Mishra, V. Increasing risk of simultaneous occurrence of flash drought in major global croplands. *Environ. Res. Lett.* **18**, 044044 (2023).
21. Liu, L. et al. Soil moisture dominates dryness stress on ecosystem production globally. *Nat. Commun.* **11**, 4892 (2020).
22. Rigden, A. J., Mueller, N. D., Holbrook, N. M., Pillai, N. & Huybers, P. Combined influence of soil moisture and atmospheric evaporative demand is important for accurately predicting US maize yields. *Nat. Food* **1**, 127–133 (2020).
23. Corak, N. K., Otkin, J. A., Ford, T. W. & Lowman, L. E. L. Unraveling phenological and stomatal responses to flash drought and

implications for water and carbon budgets. *Hydrol. Earth Syst. Sci.* **28**, 1827–1851 (2024).
24. O, S. & Park, S. K. Global ecosystem responses to flash droughts are modulated by background climate and vegetation conditions. *Commun. Earth Environ.* **5**, 1–7 (2024).
25. Jing, Y., Wang, S., Chan, P. W. & Yang, Z.-L. Gross primary productivity is more sensitive to accelerated flash droughts. *Commun. Earth Environ.* **6**, 1–10 (2025).
26. Orth, R., Destouni, G., Jung, M. & Reichstein, M. Large-scale biospheric drought response intensifies linearly with drought duration in arid regions. *Biogeosciences* **17**, 2647–2656 (2020).
27. Basara, J. B. et al. The evolution, propagation, and spread of flash drought in the Central United States during 2012. *Environ. Res. Lett.* **14**, 084025 (2019).
28. Qing, Y., Wang, S., Ancell, B. C. & Yang, Z.-L. Accelerating flash droughts induced by the joint influence of soil moisture depletion and atmospheric aridity. *Nat. Commun.* **13**, 1139 (2022).
29. Zeng, Z. et al. Increased risk of flash droughts with raised concurrent hot and dry extremes under global warming. *NPJ Clim. Atmos. Sci.* **6**, 1–12 (2023).
30. Zhang, M. et al. A pronounced decline in northern vegetation resistance to flash droughts from 2001 to 2022. *Nat. Commun.* **16**, 2984 (2025).
31. Zhang, M. & Yuan, X. Rapid reduction in ecosystem productivity caused by flash droughts based on decade-long FLUXNET observations. *Hydrol. Earth Syst. Sci.* **24**, 5579–5593 (2020).
32. Gu, L. et al. Flash drought impacts on global ecosystems are amplified by extreme heat. *Nat. Geosci.* **18**, 709–715 (2025).
33. Ho, S., Buras, A. & Tuo, Y. Comparing agriculture-related characteristics of flash and normal drought reveals heterogeneous crop response. *Water Resour. Res.* **59**, e2023WR034994 (2023).
34. Zhu, P. et al. The critical benefits of snowpack insulation and snowmelt for winter wheat productivity. *Nat. Clim. Change* **12**, 485–490 (2022).
35. Zhao, H. et al. U.S. winter wheat yield loss attributed to compound hot-dry-windy events. *Nat. Commun.* **13**, 7233 (2022).
36. Schnitkey, G. Weekly Farm Economics: Drought and Crop Insurance Loss Experience in 2012. farmdoc daily (5):51, Department of Agricultural and Consumer Economics, University of Illinois at Urbana-Champaign, March 19, (2013).
37. Seneviratne, S. et al. Changes in climate extremes and their impacts on the natural physical environment. In *Managing the Risks of Extreme Events and Disasters to Advance Climate Change Adaptation. Special Report of the Intergovernmental Panel on Climate Change* (eds. Field, C. B., Barros, V., Stocker, T. F., Qin, D., Dokken, D. J., Ebi, K. L., Mastrandrea, M. D., Mach, K. J., Plattner, G. -K., Allen, S. K., Tignor, M. & Midgley, P. M.) 109–230 (Cambridge Univ. Press, 2012).
38. Jing, L. et al. The persistent impact of drought stress on the resilience of summer maize. *Front. Plant Sci.* **14**, 1016993 (2023).
39. Zhong, Z. et al. Disentangling the effects of vapor pressure deficit on northern terrestrial vegetation productivity. Sci. Adv. **9**, eadf3166 (2023).
40. Folberth, C. et al. Parameterization-induced uncertainties and impacts of crop management harmonization in a global gridded crop model ensemble. *PLoS ONE* **14**, e0221862 (2019).
41. Chai, Y. et al. Flash droughts exacerbate global vegetation loss and delay recovery. *Nat. Commun.* **17**, 485 (2025).
42. Mohammadi, K. & Wang, G. Impact matters: Detection and early warning of agriculturally impactful flash droughts. *Bull. Am. Meteorol. Soc.* **106**, E752–E769 (2025).
43. Wang, R. et al. Onset and severity thresholds of drought impacts on wheat. *Agric. Water Manag.* **281**, 108259 (2023).
44. Wang, X. et al. Global irrigation contribution to wheat and maize yield. *Nat. Commun.* **12**, 1235 (2021).
45. Zhang, L. et al. Increased irrigation could mitigate future warming-induced maize yield losses in the Ogallala Aquifer. *Commun. Earth Environ.* **6**, 483 (2025).
46. Proctor, J., Rigden, A., Chan, D. & Huybers, P. More accurate specification of water supply shows its importance for global crop production. *Nat. Food* **3**, 753–763 (2022).
47. Heinicke, S., Frieler, K., Jägermeyr, J. & Mengel, M. Global gridded crop models underestimate yield responses to droughts and heatwaves. *Environ. Res. Lett.* **17**, 044026 (2022).
48. Dos Santos Vianna, M., Metselaar, K., De Jong Van Lier, Q., Gaiser, T. & Marin, F. R. The importance of model structure and soil data detail on the simulations of crop growth and water use: a case study for sugarcane. *Agric. Water Manag.* **301**, 108938 (2024).
49. Asseng, S. et al. Uncertainty in simulating wheat yields under climate change. *Nat. Clim. Change* **3**, 827–832 (2013).
50. Xiong, W. et al. Different uncertainty distribution between high and low latitudes in modelling warming impacts on wheat. *Nat. Food* **1**, 63–69 (2020).
51. Maestrini, B. et al. Mixing process-based and data-driven approaches in yield prediction. *Eur. J. Agron.* **139**, 126569 (2022).
52. Ren, C., He, L. & Rosa, L. Integrated irrigation and nitrogen optimization is a resource-efficient adaptation strategy for US maize and soybean production. *Nat. Food* **6**, 389–400 (2025).
53. UNDRR. *GAR* Special Report on Drought 2021. United Nations Office for Disaster Risk Reduction https://www.undrr.org/publication/gar-special-report-drought-2021 (2021).
54. Schwartz, C., Haigh, T., Svoboda, M. & Goebel, M. How is flash drought understood?—Experts' definitions and decision-makers' perceptions. *Weather Clim. Soc.* **15**, 909–924 (2023).
55. Otkin, J. A. et al. Development of a flash drought intensity index. *Atmosphere* **12**, 741 (2021).
56. DeAngelis, A. M. et al. Prediction skill of the 2012 U.S. great plains flash drought in subseasonal experiment (SubX) models. *J. Clim.* **33**, 6229–6253 (2020).
57. Vadez, V. et al. Crop traits and production under drought. *Nat. Rev. Earth Environ.* **5**, 211–225 (2024).
58. Rosales, A. Crop Progress and Condition Layers. United States Department of Agriculture (USDA) (National Agricultural Statistics Service NASS, 2021).
59. Sakamoto, T., Gitelson, A. A. & Arkebauer, T. J. MODIS-based corn grain yield estimation model incorporating crop phenology information. *Remote Sens. Environ.* **131**, 215–231 (2013).
60. Portmann, F. T., Siebert, S. & Döll, P. MIRCA2000—Global monthly irrigated and rainfed crop areas around the year 2000: a new high-resolution data set for agricultural and hydrological modeling. *Glob. Biogeochem. Cycles* **24**, https://doi.org/10.1029/2008GB003435 (2010).
61. Rosa, L., Chiarelli, D. D., Rulli, M. C., Dell'Angelo, J. & D'Odorico, P. Global agricultural economic water scarcity. *Sci. Adv.* **6**, 1–11 (2020).
62. Jägermeyr, J. et al. Climate impacts on global agriculture emerge earlier in new generation of climate and crop models. *Nat. Food* **2**, 873–885 (2021).
63. Miralles, D. G. et al. GLEAM4: global land evaporation and soil moisture dataset at 0.1° resolution from 1980 to near present. *Sci. Data* **12**, 416 (2025).
64. Muñoz-Sabater, J. et al. ERA5-Land: a state-of-the-art global reanalysis dataset for land applications. *Earth Syst. Sci. Data* **13**, 4349–4383 (2021).
65. Rodell, M. et al. The global land data assimilation system. *Bull. Am. Meteorol. Soc.* **85**, 381–394 (2004).
66. Martens, B. et al. GLEAM v3: satellite-based land evaporation and root-zone soil moisture. *Geosci. Model Dev.* **10**, 1903–1925 (2017).
67. NASA. README Document for NASA GLDAS Version 2 Data Products. https://git.earthdata.nasa.gov/projects/ECS/repos/uvg/raw/input/README_GLDAS2.pdf?at=refs%2Fheads%2Fmaster.

68. Daly, C. et al. Physiographically sensitive mapping of climatological temperature and precipitation across the conterminous United States. *Int. J. Climatol.* **28**, 2031–2064 (2008).
69. Lobell, D. B., Deines, J. M. & Tommaso, S. D. Changes in the drought sensitivity of US maize yields. *Nat. Food* **1**, 729–735 (2020).
70. Xue, J., Huete, A., Liu, Z., Gao, S. & Lu, X. A lightweight SIF-based crop yield estimation model: a case study of Australian wheat. *Agric. For. Meteorol.* **364**, 110439 (2025).
71. Ji, P. & Yuan, X. Disparities and similarities in the spatiotemporal dynamics of flash and slow droughts in China. *Environ. Res. Lett.* **19**, 084015 (2024).
72. Chen, H. & Wang, S. Compound dry and wet extremes lead to an increased risk of rice yield loss. *Geophys. Res. Lett.* **50**, e2023GL105817 (2023).
73. Hendrawan, V. S. A., Kim, W., Touge, Y., Ke, S. & Komori, D. A global-scale relationship between crop yield anomaly and multiscalar drought index based on multiple precipitation data. *Environ. Res. Lett.* **17**, 014037 (2022).
74. Chen, T & He, T. xgboost: Extreme Gradient Boosting. 1.7.11.1 https://doi.org/10.32614/CRAN.package.xgboost (2014).
75. Li, Z. Extracting spatial effects from machine learning model using local interpretation method: An example of SHAP and XGBoost. *Comput. Environ. Urban Syst.* **96**, 101845 (2022).
76. Nalluri, M., Pentela, M. & Eluri, N. R. A scalable tree boosting system: XG boost. *Int. J. Res. Stud. Sci. Eng. Technol.* **7**, 36–51 (2020).
77. Frieler, K. et al. Scenario setup and forcing data for impact model evaluation and impact attribution within the third round of the Inter-Sectoral Impact Model Intercomparison Project (ISIMIP3a). *Geosci. Model Dev.* **17**, 1–51 (2024).
78. Jägermeyr, J. & Frieler, K. Spatial variations in crop growing seasons pivotal to reproduce global fluctuations in maize and wheat yields. *Sci. Adv.* **4**, 1–10 (2018).
79. Schewe, J. et al. State-of-the-art global models underestimate impacts from climate extremes. *Nat. Commun.* **10**, 1005 (2019).
80. Müller, C. et al. The Global Gridded Crop Model Intercomparison phase 1 simulation dataset. *Sci. Data* **6**, 50 (2019).
81. Martínez-Fernández, J., González-Zamora, A., Sánchez, N., Gumuzzio, A. & Herrero-Jiménez, C. M. Satellite soil moisture for agricultural drought monitoring: assessment of the SMOS derived Soil Water Deficit Index. *Remote Sens. Environ.* **177**, 277–286 (2016).
82. Alfieri, L., Burek, P., Feyen, L. & Forzieri, G. Global warming increases the frequency of river floods in Europe. *Hydrol. Earth Syst. Sci.* **19**, 2247–2260 (2015).

Acknowledgements

We are particularly grateful to all members of the Hydroclimate Extremes Lab at The Hong Kong Polytechnic University for their valuable suggestions and constructive discussions during the development of this work.

Author contributions

S.W. and C.Q. designed the study. C.Q. carried out the analysis and drafted the manuscript. S.W. supervised the analysis and contributed to the interpretation and discussion of the results. P.Z., J.A.O., Z.L.Y., and A.A. provided comments and suggestions for improving the quality of this manuscript. All authors revised and edited the manuscript.

Funding

S.W. discloses support for the research and publication of this work from the Research Grants Council of the Hong Kong Special Administrative Region, China (Project No. PolyU/RGC 15232023), the Otto Poon Research Institute for Climate-Resilient Infrastructure (Project No. P0055919), and the State Key Laboratory of Climate Resilience for Coastal Cities at The Hong Kong Polytechnic University. C.Q., P.Z., J.A.O., Z.L.Y., and A.A. declare no relevant funding.

Competing interests

The authors declare no competing interests.

Additional information

Supplementary information The online version contains supplementary material available at https://doi.org/10.1038/s43247-026-03834-z.

Correspondence and requests for materials should be addressed to Shuo Wang.

Peer review information *Communications Earth & Environment* thanks Lina Zhang and Miguel Lovino for their contribution to the peer review of this work. Primary handling editors: Wenfeng Liu, Mengjie Wang. A peer review file is available.

Reprints and permissions information is available at http://www.nature.com/reprints

Publisher's note Springer Nature remains neutral with regard to jurisdictional claims in published maps and institutional affiliations.

Open Access This article is licensed under a Creative Commons Attribution-NonCommercial-NoDerivatives 4.0 International License, which permits any non-commercial use, sharing, distribution and reproduction in any medium or format, as long as you give appropriate credit to the original author(s) and the source, provide a link to the Creative Commons licence, and indicate if you modified the licensed material. You do not have permission under this licence to share adapted material derived from this article or parts of it. The images or other third party material in this article are included in the article's Creative Commons licence, unless indicated otherwise in a credit line to the material. If material is not included in the article's Creative Commons licence and your intended use is not permitted by statutory regulation or exceeds the permitted use, you will need to obtain permission directly from the copyright holder. To view a copy of this licence, visit http://creativecommons.org/licenses/by-nc-nd/4.0/.

© The Author(s) 2026